Indium surface diffusion on InAs (2×4) reconstructed wetting layers on GaAs(001)

Marcello Rosini,[1,*] Maria Clelia Righi,[1] Peter Kratzer,[2] and Rita Magri[1]

[1]*Dipartimento di Fisica, Università degli Studi di Modena e Reggio Emilia and S3 Research Center of CNR-INFM, via Campi 213/A, 41100 Modena, Italy*

[2]*Fachbereich Physik, Universität Duisburg-Essen, Lotharstrasse 1, 47048 Duisburg, Germany*

(Received 31 March 2008; revised manuscript received 4 September 2008; published 2 February 2009)

In this paper we present a study of In surface diffusion on InAs wetting layers deposited on the (001) surface of GaAs. The $\alpha_2(2\times4)$ and $\beta_2(2\times4)$ reconstructions stabilized by a high In concentration are considered. The low symmetry of the $\alpha_2(2\times4)$ reconstruction allowed us to understand the effect of the wetting-layer symmetry on the adsorbate diffusion. We find that (i) the diffusion coefficient value is larger for In motion on the α_2 reconstruction than on the β_2 reconstruction. This is due to the presence on β_2 of an additional As dimer that rises locally the potential energy surface and offer an additional site to which the In adatom can bind strongly. (ii) The In adsorption sites located within the As dimers have to be taken into account properly for these specific reconstructions, since they greatly affect the value of the diffusion coefficient. This is in contrast to what happens for the other reconstructions reported in the literature. (iii) The adsorbate diffusion is highly anisotropic with the $[\bar{1}10]$ direction favored over the [110] direction, due to the presence of low-potential channels along $[\bar{1}10]$. (iv) The anisotropy is slightly smaller on the α_2 reconstruction than on the β_2 reconstruction because on the β_2 there is an additional diffusion channel along the $[\bar{1}10]$ direction.

DOI: 10.1103/PhysRevB.79.075302 PACS number(s): 68.43.Jk, 31.50.−x

I. INTRODUCTION

A first step for understanding nucleation of self-assembled quantum dots (QDs) is to investigate what happens during the mass transport taking place at the two-dimensional to three-dimensional 2D→3D transition. Here we address the Stranski-Krastanov growth mode[1] typical of the InAs/GaAs quantum dot system. The coordinated adsorbate motion during mass transport is determined by an ensemble of single surface diffusion events.[2] Thus, the understanding of surface diffusion is fundamental for shedding light on the nucleation mechanism and to determine the final dot density and arrangement.

Adsorbate surface diffusion takes place on reconstructed InGaAs (001) wetting layers (WL) and depends on the growth conditions. In this paper we refer to molecular-beam epitaxy (MBE) growth conditions, mainly, through the choice of the particular surface reconstructions (depending on the As chemical potential) and of the growth temperature.

Since we are interested in In diffusion at the onset of the 2D→3D transition, we focus our attention mainly to particularly In-rich WLs, with a (2×4) (001) surface reconstruction, which was reported in the literature[2–5] as the observed reconstruction of the WL at the onset of quantum dot formation. The transition takes place at $\theta\approx1.7$ ML coverage, with $x=0.8$ In surface composition.[6,7] For a (001) In-rich surface, the stable (2×4) reconstructions are α_2 and β_2.[8–10] The β_2 presents an additional As dimer; thus it is stabilized in richer As atmosphere or/and at a lower growth temperature where As evaporation from the surface diminishes. In this paper we determine the properties of In surface diffusion considering the α_2 and β_2 reconstructions for an In-rich WL grown on GaAs. It has been found[11] that as the In coverage increases, the (001) surface reconstruction changes from $c(4\times4)$ for pure GaAs to (2×3) at an In $\theta\approx0.7$ coverage and finally to a (2×4) reconstruction at a much higher In coverage. The characteristics of In adsorption have been previously studied for the $c(4\times4)$ GaAs(001),[10] the (1×3) and $(2\times3)$$In_{0.66}Ga_{0.33}As(001)$,[12] and for the α_2 and $\beta_2(2\times4)$ InAs/GaAs(001) (Ref. 13) WLs. Here, we add a further piece to the picture of In diffusion on these InGaAs WLs, reporting the results of In diffusion on (2×4) reconstructed surfaces.

Our description of In diffusion is based on the transition state theory.[14–16] In adatoms perform thermally activated jumps from an adsorption site on the WL to another one, overcoming energy barriers. The In adsorption sites on the α_2 and β_2 reconstructed WLs and the corresponding diffusion energy barriers have been previously calculated by us using a first-principles pseudopotential density-functional theory (DFT) approach, in the local-density approximation (LDA).[13] We know that the As dimers (ad-dimers) at the top of the surface and the As dimers (indimers) in the trench—two atomic layers below—give rise to higher-potential regions for the In adatom that define low-potential channels along the $[\bar{1}10]$ direction. Similar results were obtained for the β_2 surface reconstruction, where an additional As ad-dimer is present on the top of the surface. These results are here used as a starting point to calculate the properties of In diffusion. The analysis of the In trajectories on the WL, with the indication of which among the adsorption sites has the highest probability to be visited by the adsorbate and which one binds the adsorbate for a longer time, can provide useful information for a later investigation of the nucleation process.

The paper is organized as follows. In Sec. II we describe the theoretical methods used to study In diffusion and calculate the diffusion coefficient. Section III reports our results for the diffusion on the (2×4) reconstructed (001) InGaAs covered surfaces using (i) an analytical solution of the diffusion master equation and (ii) direct kinetic Monte Carlo (kMC) simulations. The results are discussed in detail and compared with the existing literature. Finally, in Sec. IV, we summarize and conclude.

II. METHOD

The tracer diffusion tensor is defined as[17–19]

$$D^*_{\alpha,\beta} = \lim_{t\to\infty} \frac{1}{4t} \langle \Delta r_\alpha(t) \Delta r_\beta(t) \rangle, \tag{1}$$

where $\Delta r_{\alpha(\beta)}(t)$ is the adsorbate displacement with respect to the initial position, along the coordinate α (β) (we use Greek letters to indicate tensor in-plane components x and y). In the case of isotropic surface diffusion, it will be $D^*_{\alpha,\beta}=D^*\delta_{\alpha,\beta}$, where D^* is the tracer diffusion coefficient. It is important to note that the definition [Eq. (1)] applies only to the random walk of an isolated adatom: the so-called *tracer*. This condition corresponds to an experimental situation of low adatom concentration and vanishing interaction among the adatoms.

The diffusion motion originates from the random walk of the adsorbate on the surface, consisting of a series of thermally activated jumps. The adsorbate in an initial adsorption state (j) after a given time τ escapes to another adsorption site (k) with a transition probability per unit time $\Gamma_{kj} \equiv \Gamma_{k\leftarrow j} \equiv 1/\tau_{kj}$. It is clear that the tracer diffusion coefficient is a function of the whole set of Γ_{kj}.

In order to determine the coefficients Γ_{kj}, we apply the transition state theory.[14–16] Thus, the transition probability per unit time is expressed as:

$$\Gamma_{kj} = \Gamma^{(0)}_{kj} e^{-\Delta U/k_B T}, \tag{2}$$

where ΔU is the difference between the $T=0$ K energy of the adsorption site i and that of the transition state at the saddle point along the path $j\to k$ that is commonly referred to as diffusion barrier. $\Gamma^{(0)}_{kj}$ is interpreted as the attempt-to-escape frequency of the adatom in site i and it is related to the vibrational properties of the system and to the temperature. In this work we consider $\Gamma^{(0)}_{kj}=\Gamma_0=10^{13}$ s^{-1}, for each j and k. This is a reasonable assumption since, in general, in most cases of single adatom hopping diffusion, the prefactor $\Gamma^{(0)}_{kj}$ has been found to have a maximum variation of a factor 2.[20] The determination of ΔU is more critical since it appears in the exponent of Eq. (2). The energy barriers ΔU that enter the process rates [Eq. (2)] are those calculated from first principles.[13]

To calculate the diffusion tensor we follow two distinct ways: (i) the analytical solution of the master equation for the random walk and (ii) the kinetic Monte Carlo simulation of the diffusion kinetics.

A. Solution of the master equation of a 2D random walk

We write the master equation for the probability,

$$\frac{d}{dt}P_j(\mathbf{n},t) = \sum_{\substack{k=1\\k\neq j}}^{N_a} \sum_{\mathbf{n}'} \Gamma_{jk}(\mathbf{n}-\mathbf{n}')P_k(\mathbf{n}',t) - P_j(\mathbf{n},t)\sum_{\substack{k=1\\k\neq j}}^{N_a} \sum_{\mathbf{n}'} \Gamma_{kj}(\mathbf{n}'-\mathbf{n}), \tag{3}$$

where $P_j(\mathbf{n},t)$ is the probability of finding the random walker in the adsorption site j of the $\mathbf{n}$th unit cell at time t, and $\mathbf{n}=(n_x,n_y)$ is the 2D lattice index along the directions x and y. $\Gamma_{kj}(\mathbf{n}'-\mathbf{n})$ is the transition probability per unit time from site $(j,\mathbf{n})$ to site $(k,\mathbf{n}')$. N_a is the number of adsorption sites per surface unit cell. The conditions $P_j(\mathbf{n},t)\in[0,1]$ and $\Sigma_{j=1}^{N_a}\Sigma_{\mathbf{n}}P_j(\mathbf{n},t)=1$ hold. The first term represents the adatom coming from sites k to site j; the second one represents the adatom leaving j by jumping to all the other possible sites k.

By applying the Fourier transform $P_j(\mathbf{n},t)=\Sigma_{\mathbf{q}}e^{i\mathbf{q}\mathbf{n}}P_j(\mathbf{q},t)$, the master equation (3) can be brought to the compact form

$$\frac{d}{dt}\mathbf{P}(\mathbf{q},t) = \Gamma(\mathbf{q})\mathbf{P}(\mathbf{q},t), \tag{4}$$

where $\mathbf{P}$ is the array of N_a elements of the probability Fourier coefficients and Γ is a $N_a\times N_a$ matrix whose elements are

$$\Gamma_{jk}(\mathbf{q}) = \sum_{\mathbf{n}} e^{i\mathbf{q}\mathbf{n}}\Gamma_{jk}(\mathbf{n}) - \delta_{jk}\sum_{l=1}^{N_a}\sum_{\mathbf{n}}\Gamma_{lj}(\mathbf{n}) \tag{5}$$

commonly referred to as the transition rate matrix.[21]

We are now interested in the steady-state solutions of Eqs. (3) and (4). Owing to the periodic boundary conditions and considering a very large system with an infinite number N of cells, $P_j(\mathbf{q})=0$ for each $\mathbf{q}\neq 0$. The steady-state solution for the P_j is calculated directly from

$$\Gamma(\mathbf{q}=0)\mathbf{P}(\mathbf{q}=0) = 0. \tag{6}$$

Another useful quantity for understanding diffusion is the occupation frequency for each site f_j that can be calculated as

$$f_j = P_j/\tau_j, \tag{7}$$

where τ_j is the mean permanence time in each site, given by the sum of the probabilities of escaping from site j,

$$\frac{1}{\tau_j(\mathbf{n})} = \sum_{k=1}^{N_a}\sum_{\mathbf{n}'}\Gamma_{kj}(\mathbf{n}'-\mathbf{n}). \tag{8}$$

The tracer diffusion tensor can be obtained[22,23] from the eigenvalues of the transition rate matrix [Eq. (5)]. It can be demonstrated[24] that for this master equation there is one and only one eigenvalue; let it be $\gamma_1(\mathbf{q})$, such that $\gamma_1(0)=0$ and the real part of all the other eigenvalues is negative. The tracer diffusion tensor is obtained as

$$\mathbf{D}^* = \mathbf{B}\mathbf{H}\mathbf{B}^T, \tag{9}$$

where $\mathbf{B}$ is the transformation matrix from Cartesian coordinates to lattice indexes, and $\mathbf{H}$ is the Hessian of the above eigenvalue,

$$\mathbf{H} = -\frac{1}{2}\nabla_{\mathbf{q}}\nabla_{\mathbf{q}}\gamma_1(\mathbf{q})|_{\mathbf{q}=0}. \tag{10}$$

To calculate the diffusion properties of the In adsorbate, we have fully solved Eq. (10) without approximations.

B. Kinetic Monte Carlo simulation

The kMC algorithm[25–29] provides a numerical solution to the Markovian master equation (3) and allows to simulate the

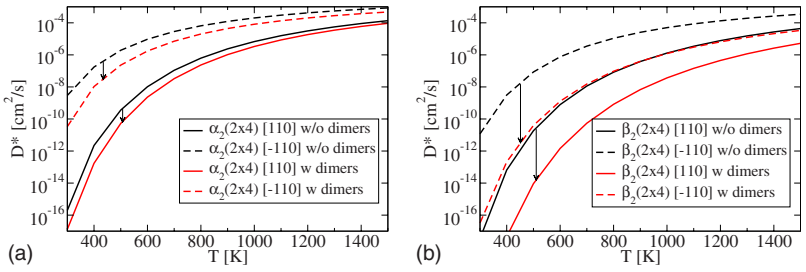

FIG. 1. (Color online) Diffusion coefficients for $\alpha_2(2\times4)$ and $\beta_2(2\times4)$. Solid lines refer to the [110] direction and dashed lines to the $[\bar{1}10]$ direction. Red (light) and black (dark) lines are calculated with and without the adsorbate inclusion in the dimers, respectively. The arrows evidence the change in the coefficients when the sites in the dimers are included in the calculation.

system kinetics over large time scales. The surface diffusion process involves macroscopic time scales because it is ruled by rare events. Rare events, such as the jumps from site to site of a diffusing adatom, occur when the system undergoes a sudden transition—usually thermally activated—from one stable phase-space region to another one. The time interval between these transitions is several orders of magnitude higher than the time period of atom vibrations around their equilibrium positions. Thus, an atomistic description of the physical phenomena governed by rare events, such as surface-atom diffusion and dot growth, cannot be achieved by a straightforward use of molecular dynamics. The kMC method combined with the first-principles calculation of the activation energies of rare events constitutes a powerful approach to simulate the time evolution of these phenomena, including atomistic information. This is achieved by coarse graining the particle dynamics to the rare events which rules the system evolution, while averaging over the short-time dynamics of atom vibrations.

We adopted the kMC algorithm to calculate the trajectories followed by an In adatom when diffusing on the α_2 and β_2 reconstructed (001) surfaces of the InAs WL at different temperatures. In our simulations the particle moves on a discrete lattice where the sites correspond to the metastable adatom configurations previously identified by means of first-principles calculations.[13] The particle jumps occur with the rates defined by the transition state theory in the harmonic approximation (2).

At the beginning of the kMC simulation, the In adatom is deposited on a randomly selected lattice site. Then a loop consisting of the following four steps is executed: (i) the total rate R for In diffusion is calculated by summing up the rates of all the hopping processes that are possible starting from the selected adatom position [as in Eq. (8)]; (ii) a particular diffusion event (say l) is randomly selected with a probability given by Γ_l/R; (iii) the event is executed, i.e., the occupations of the starting and the arrival sites of the atomic jump are changed; and (iv) the time is updated by an increment dt that is a random variable with the Poisson distribution and average value $\langle dt\rangle = 1/R$. This condition makes the kMC time a physical quantity and allows to map the simulation time with the real time. Thus, as an outcome of the kMC simulation, we obtained the trajectories that the In adatom indeed spans when diffusing at different temperatures on the reconstructed InGaAs WL surface. By "observing" the adatom wandering on the surface, we can get insight into the microscopic mechanisms at the basis of the calculated adatom diffusivity, and in particular, into the role played by the reconstruction morphology in "shaping" the adatom trajectory. By accumulating, during the simulation—the time intervals spent by the adatom in each site and the number of visits to that site—the mean permanence time is straightforwardly calculated as the ratio between the two quantities. By postprocessing the adatom trajectories, the adatom mean-square displacement is calculated as a function of time.[30] By applying the definition of Eq. (1), we extract the adatom diffusion coefficient.

III. RESULTS

In order to calculate the diffusion tensor, we identify all the possible transitions from site j to the other sites k on the surface and find the transition probabilities per unit time $\Gamma_{kj}(\mathbf{n}'-\mathbf{n})$ [Eq. (2)]. We consider only first-order transitions, i.e., transitions involving the crossing of only one saddle point in the PES. This is a reasonable approximation since the probability of higher-order transitions is of orders of magnitude smaller. In this approximation we consider the transition network relative to each reconstruction.

We consider two different situations. In the first case we exclude from the transition network the adsorption sites having the In adsorbate inserted in the As dimers; in the second case, for α_2 and β_2 also these additional adsorption sites[13] are considered, in analogy to what has been done in some previous works,[10,31,32] where the adsorbate inclusion into the dimers is found to be responsible for a strong modification of the PES and—as a consequence—of a decrease in the diffusion. In particular, these sites have been considered in the case of Ga adsorption on $\beta_2(2\times4)$.[31] In the case of In on $c(4\times4)$ (Ref. 12) and on the (1×3) and (2×3) (Ref. 10) surfaces, the authors have found these sites too shallow, with a low probability to be occupied at usual growth temperatures, and thus they have not been inserted in the diffusion calculation. In our case the binding sites into the As dimers cannot be neglected, since the barrier on the PES to be overcome by the random walker for breaking the As dimers and inserting into them are few hundreds of meV, comparable to the other barriers on the PES.[13] Thus, according to Eq. (2), the probability to observe such events during surface diffusion is important and can strongly affect surface diffusion.

A. Master-equation solution

Here we discuss the results obtained from the master equation following the procedure described in Sec. II A.

The diffusion coefficients of In on the two surface reconstructions are reported in Fig. 1, with and without considering the possibility for the adsorbate to insert into the As dimers. We first notice that there is a great difference between the diffusion along the two surface directions. The

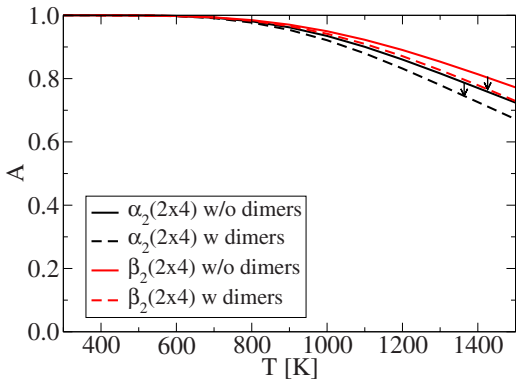

FIG. 2. (Color online) Indium diffusion anisotropy [Eq. (11)] calculated for α_2 (black lines) and for β_2 (red lines) surface reconstructions with (dashed lines) and without (solid lines) the adsorbate included in the dimers. The arrows evidence the change in the coefficients when the sites in the dimers are included

diffusion of the adsorbate is much larger along the $[\bar{1}10]$ direction, with respect to the $[110]$ direction, for both surface reconstructions. This is a consequence of the PES shape:[13] low-energy regions, with weak energy barriers extending along the $[\bar{1}10]$ direction, act as deep channels for In motion, while along the orthogonal $[110]$ direction, the adsorption sites are separated by higher barriers corresponding to the As dimers. This difference can be quantitatively evaluated by defining the anisotropy,

$$A = \frac{D^*_{[\bar{1}10]} - D^*_{[110]}}{D^*_{[\bar{1}10]} + D^*_{[110]}}. \tag{11}$$

The anisotropy calculated for both surfaces is given in Fig. 2. Of course the anisotropy is higher at low temperatures because the probability to overcome high barriers is lower than at high temperatures; thus at low T the adsorbate diffusion occurs mainly along $[\bar{1}10]$. This means that the material transport toward the quantum dots (and, likewise, transport away from the quantum dots during overgrowth by a capping layer) occurs preferentially along the $[\bar{1}10]$ directions. Indeed, a degradation of the quantum dots leading to a pronounced elongation along $[\bar{1}10]$ has been clearly observed during slow-rate overgrowth of large InAs QDs by a GaAs capping layer.[33] Furthermore, atomic force microscopy (AFM) studies of the wetting layer below the critical coverage find the formation of large-scale anisotropic mounds elongated along the $[\bar{1}10]$ direction.[34] Both phenomena may well be related with the diffusion anisotropy we have calculated in this work.

TABLE I. Effective diffusion barriers ΔE^* (meV) along the two orthogonal $[110]$ and $[\bar{1}10]$ surface directions.

Surface	$\Delta E^*_{[110]}$	$\Delta E^*_{[\bar{1}10]}$
InAs WL $\alpha_2(2\times4)$ without dimer	827	405
InAs WL $\beta_2(2\times4)$ without dimer	971	554
InAs WL $\alpha_2(2\times4)$ with dimer	958	525
InAs WL $\beta_2(2\times4)$ with dimer	1033	893

When we insert in the transition network the adsorption sites located between the two As atoms of the dimers, the diffusion coefficient is, in general, highly reduced, since the new sites that are deep and surrounded by high barriers (of the order of 600–900 meV) act as traps for the diffusing adatom. The reduction in the In diffusion is more relevant on β_2 than on α_2 since, in the former case, the number of these additional adsorption sites is obviously larger. The anisotropy is instead slightly reduced for both reconstructions at high temperatures. Thus, we see that the anisotropy of the diffusion tensor for α_2 and β_2 is similar.

A further quantity we want to evaluate is the effective diffusion barrier ΔE^* along a specified direction. It is obtained from the Arrhenius plot of the diffusion coefficient along specific direction α,

$$D^*_\alpha \propto e^{-\Delta E^*/k_B T}. \tag{12}$$

The effective diffusion barrier gives an indication of the diffusion efficiency along the direction α. In Table I our results for ΔE^* are reported. We notice that the (2×4) reconstructions of the InAs WL studied in this work present high effective diffusion barriers, with the barriers of β_2 slightly higher than those of α_2. As expected, when considering the adsorbate inclusion into the dimer-breaking adsorption sites, the effective diffusion barriers considerably increase.

The analysis of the site mean occupation time τ_j [(Eq. (8) and Fig. 3)] reveals that the sites where the adsorbate spends most of its time are the ones where the In adsorbate is included in the dimers. Other important high-permanence sites are A_2 and A_4 for the α_2 surface reconstruction and A_6 and A_8 for the β_2 reconstruction.[13] The average permanence time τ_j in the dimer sites is about 3 orders of magnitude higher than that in the other sites, owing to the higher-confining barriers. This demonstrates the need of including these sites into the transition network, for a correct description of the diffusion

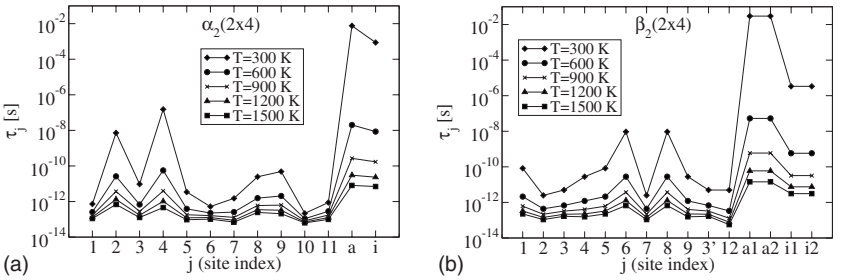

FIG. 3. Mean permanence time τ_j for each site, for α_2 and for β_2, at different substrate temperatures. The additional sites where the In adatom is included in the dimer are labeled by "a" and "i".

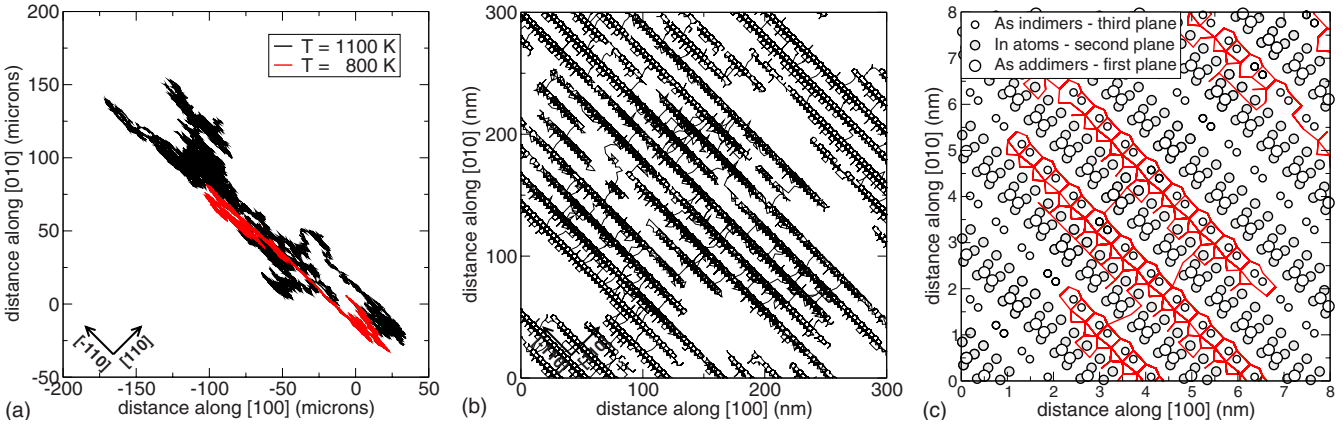

FIG. 4. (Color online) In adatom trajectory covered in 0.01 s when diffusing on the α_2 reconstruction, at (a) two different temperatures. The trajectory corresponding to $T=1100$ K [represented in black in panel (a)] is zoomed onto the nanometer scale in panels (b) and onto the atomic scale in panel (a).

kinetics of the In adatom on these surfaces. This property allows us to consider these sites as the best candidates for the study of the nucleation process, being the permanence time a condition for nucleation. When the temperature is increased, the permanence times tend to become similar for all adsorption sites because the thermal energy of the adsorbate is higher and the probability to overcome the barriers increases significantly everywhere.

We have found that the frequency f_j [Eq. (7)] at which each site is visited is higher for the lowest-energy adsorption sites. Regarding the site-occupation probability P_j [Eq. (8)], the solution of the master equation has been confirmed to follow the Maxwell-Boltzmann thermal distribution. This means that the occupation probability of each adsorption site is proportional to e^{-E/k_BT}, where E is the binding energy of the site. Again, we notice that the adsorption sites within the dimers show an occupation probability of about 1 order of magnitude higher than that of the other sites because of their large adsorption energy.

Our results show two interesting effects. The comparison between the In surface diffusion properties on α_2 and β_2 reveals the effects due to (i) the surface symmetry, which is lower on α_2 than on β_2, and (ii) the abundance of As on the surface. As for the symmetry effects, we find that the (110) mirror symmetry of β_2 introduces an additional binding site inside the indimer (i2) (see Figs. 8 and 10 in Ref. 13). Moreover, the symmetry break in α_2 by changing the properties of the symmetry-coupled binding sites (Fig. 5 of Ref. 13) leads to higher diffusion coefficients and a diminished anisotropy. As for the trend with the As fraction present on the surface, we see that the β_2 reconstructed WL, which has stoichiometry 0.25 of As, against a stoichiometry of 0 of α_2, shows a reduced diffusion coefficient. This behavior correctly reproduces an observed trend, in which the mobility of the In adatom is found to reduce when the growing surface is exposed to a higher As flux at fixed temperature.[35] We show in this paper that this is very likely due to the increase in the number of As dimers on the surface, which increase locally the PES and offers very stable binding sites for the wandering In adatom.

B. Kinetic Monte Carlo results

As anticipated, we complemented our study on In diffusion at the (001) surface of the InGaAs WL by performing kMC simulations. These simulations besides offering the possibility to double check the analytically calculated diffusion coefficients and the mean permanence times (whose values are found to be in agreement with those calculated analytically) allow us to visualize the trajectories covered by the In adatom on a macroscopic time scale. By analyzing the features of the calculated trajectories, some information on the role played by the reconstruction in influencing the diffusion can be derived. The snapshots of the trajectories covered in 0.01 s by the In adatom when diffusing on the α_2 and on the β_2 reconstructed surfaces are displayed in Figs. 4(a) and 5(a), respectively. Two different temperatures, namely, $T=1100$ K and $T=800$ K, are considered. The higher-temperature trajectory is zoomed onto a length scale of 2 orders of magnitude smaller in the (b) panels of both the figures, while a further magnification onto the atomic scale is reported in panels (c).

When comparing the length scale of Figs. 4(a) and 5(a), it appears evident that In diffusion is higher on the α_2 reconstruction than on the β_2 one. This observation, in agreement with the diffusion coefficients (Fig. 1) and the effective barriers (Table I) calculated for the two reconstructions, may suggest that In diffusion on the (2×4) reconstructed surfaces can be reduced by increasing the As coverage. This can be done by reducing the temperature, thus limiting As desorption from the surface. A temperature decrease causes a further reduction in the In diffusion as it is clearly visible if one compares the extension of the black and the red spots displayed in panels (a), representing the adatom trajectory at $T=1100$ K and $T=800$ K, respectively.

A peculiar feature of the trajectories displayed both in Figs. 4(a) and 5(a) is represented by their marked elongation, especially at low temperature, along the $[\bar{1}10]$ direction. This feature reflects the calculated diffusion anisotropy (Fig. 2). A closer inspection at the adatom trajectories [panels (b)] reveals that the adatom diffusion on both the α_2 and the β_2

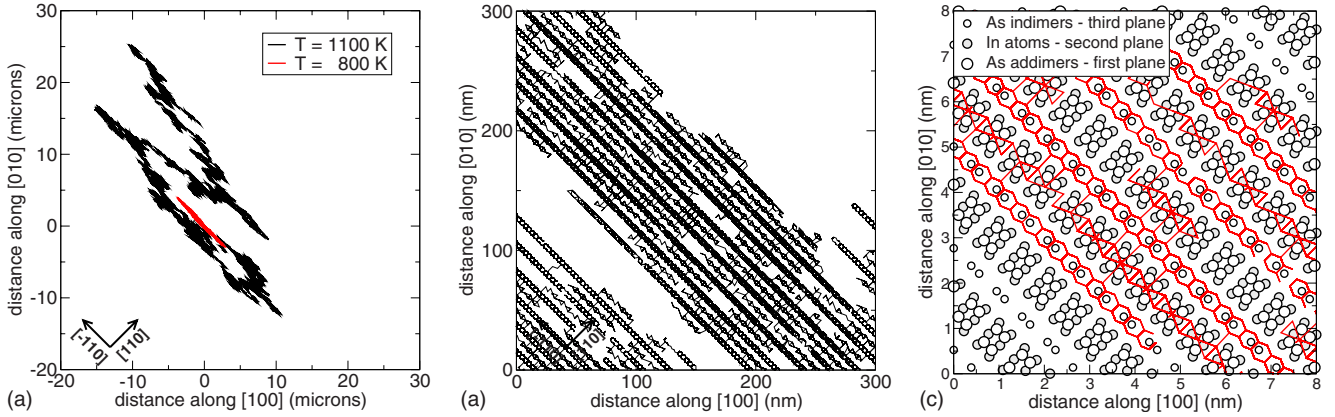

FIG. 5. (Color online) In adatom trajectory covered in 0.01 s when diffusing on the β_2 reconstruction, at (a) two different temperatures. The trajectory corresponding to $T=1100$ K [represented in black in panel (a)] is zoomed onto the nanometer scale in panels (b) and onto the atomic scale in panel (c). Note the different scales of panel (a) compared to Fig. 4(a).

surfaces consists of a series of straight paths of different lengths running along the $[\bar{1}10]$ direction, which is the direction of the surface trenches containing the As indimers and of the surface mountains containing the As ad-dimers [see panels (c)]. The diffusion along the [110] direction occurs thanks to adatom jumps from one straight path to a neighboring one. By comparing the zoomed trajectories [panels (b) and (c)] it appears evident that on the α_2 reconstruction (Fig. 4) the In diffusion occurs mainly within the trench, while on the β_2 reconstruction (Fig. 5) In diffusion occurs both within the trenches and the mountains. Thus, the β_2 reconstruction presents additional diffusion channels midway between the trenches channels. The presence of a denser arrangement of channels of high diffusivity along the $[\bar{1}10]$ direction may explain the higher diffusion anisotropy calculated for the β_2 reconstruction. Due to the presence of different diffusion channels, we may expect that the two reconstructions play a different role in determining the location and the features of the first critical nuclei.

Also, from the analysis of panels (c), we can see the effect on the In trajectories at the atomic level of loss of the mirror symmetry in the $[\bar{1}10]$ in the α_2 reconstruction with respect to the β_2 reconstruction.

IV. CONCLUSIONS

The diffusion coefficient has been evaluated for In on $\alpha_2(2\times4)$ and $\beta_2(2\times4)$ InAs WLs on GaAs. The α_2 and β_2 reconstructions are stabilized by a high In coverage. The energy barriers for the diffusion have been extracted from the *ab initio* calculated PESs and from them the corresponding diffusion coefficients have been derived.

First, we compare the diffusion properties of the In adatom on the α_2 and on the $\beta_2(2\times4)$ reconstructed WLs. We find that the diffusion coefficient is larger for the α_2 reconstruction, which has one less As dimer, with respect to the β_2 reconstruction. We have found that one reason for the lower diffusion coefficient on β_2 is related to the existence of strongly bonded adsorption sites on these reconstructed (2×4) surfaces, which are placed inside the As surface dimers, and β_2 has one more of these sites than α_2. Also, in general, the effective barriers calculated for β_2 are higher than those calculated for α_2, since the As dimers on the surface tend to rise locally the PES introducing larger barrier regions. Our study shows that the inclusion in the adatom transition network of the highly stable adsorption sites within the As dimers has a relevant effect on the diffusion coefficient, decreasing noticeably its value.

Also we find that In diffusion on α_2 and β_2 is highly anisotropic with the $[\bar{1}10]$ direction favored over the [110] orthogonal direction. This is due to the existence of low-potential channels extending along the $[\bar{1}00]$ direction, with lower barriers favoring the In adatom motion. Our calculated anisotropy can be related to experimental observations of elongated shapes along $[\bar{1}10]$ when growing or overgrowing InGaAs quantum dots.

Comparing α_2 and β_2, we found that the diffusion anisotropy is higher in the case of β_2. This behavior has been explained by analyzing the diffusing In adatom trajectories on both reconstructions. The β_2 reconstruction presents an additional potential channel along the $[\bar{1}10]$ direction per surface unit cell that—differently from the usual indimer trenches [Fig. 4(b)]—which are also present on the α_2, is located in the As ad-dimer mountains [Fig. 5(b)]. The presence of different surface regions explored by the diffusing In adatom may result in a different location and arrangement of the first critical nuclei on the α_2 and β_2 WL reconstructions.

ACKNOWLEDGMENTS

We acknowledge the support of the MIUR PRIN-2005, Italy. The calculations were performed at CINECA-Bologna under the grant "Iniziativa Calcolo Parallelo del CNR-INFM" and at LabCsai in Modena.

*marcello.rosini@unimore.it

[1] I. N. Stranski and L. Kastranow, Sitzungsber. Akad. Wiss. Wien, Math.-Naturwiss. Kl., Abt. 2B **146**, 797 (1938).
[2] F. Patella, F. Arciprete, E. Placidi, S. Nufris, M. Fanfoni, A. Sgarlata, D. Schiumarini, and A. Balzarotti, Appl. Phys. Lett. **81**, 2270 (2002).
[3] N. Grandjean and J. Massies, J. Cryst. Growth **134**, 51 (1993).
[4] P. A. Bone, J. M. Ripalda, G. R. Bell, and T. S. Jones, Surf. Sci. **600**, 973 (2006).
[5] J. G. Belk, C. F. McConville, J. L. Sudijono, T. S. Jones, and B. A. Joyce, Surf. Sci. **387**, 213 (1997).
[6] F. Patella, F. Arciprete, M. Fanfoni, and A. Balzarotti, Appl. Phys. Lett. **88**, 161903 (2006).
[7] F. Patella, F. Arciprete, M. Fanfoni, V. Sessi, and A. Balzarotti, Appl. Phys. Lett. **87**, 252101 (2005).
[8] C. Ratsch, Phys. Rev. B **63**, 161306(R) (2001).
[9] P. Kratzer, E. Penev, and M. Scheffler, Appl. Surf. Sci. **216**, 436 (2003).
[10] E. Penev, P. Kratzer, and M. Scheffler, Phys. Rev. B **64**, 085401 (2001).
[11] J. G. Belk, C. F. McConville, J. L. Sudijono, T. S. Jones, and B. A. Joyce, Surf. Sci. **387**, 213 (1997).
[12] E. Penev, S. Stojkovic, P. Kratzer, and M. Scheffler, Phys. Rev. B **69**, 115335 (2004).
[13] M. Rosini, R. Magri, and P. Kratzer, Phys. Rev. B **77**, 165323 (2008).
[14] P. Pechukas, in *Dynamics of Molecular Collisions: Part B*, edited by W. H. Miller (Plenum, New York, 1976).
[15] D. G. Truhlar, W. L. Hase, and J. T. Hynes, J. Phys. Chem. **87**, 2664 (1983).
[16] D. G. Truhlar, B. C. Garret, and S. J. Klipenstein, J. Phys. Chem. **100**, 12771 (1996).
[17] R. Gomer, Rep. Prog. Phys. **53**, 917 (2002).
[18] *Interaction of Atoms and Molecules with Solid Surfaces*, edited by V. Bortolani, N. H. March, and P. Tosi (Plenum, New York, 1990).
[19] *Surface Mobility on Solid Materials*, NATO Advanced Studies Institute, Series B: Physics, edited by V. T. Binh (Plenum, New York, 1983), Vol. 86.
[20] C. Ratsch and M. Scheffler, Phys. Rev. B **58**, 13163 (1998).
[21] J. W. Haus and K. W. Kehr, Phys. Rep. **150**, 263 (1987).
[22] R. Festa and E. Galleani, Physica A **90**, 229 (1978).
[23] M. v. Smoluchowski, Ann. Phys. **48**, 1103 (1915).
[24] J. Schnakenberg, Rev. Mod. Phys. **48**, 571 (1976).
[25] A. B. Bortz, M. H. Kalos, and J. L. Lebowitz, J. Comput. Phys. **17**, 10 (1975).
[26] D. T. Gillespie, J. Comput. Phys. **22**, 403 (1976).
[27] A. F. Voter, Phys. Rev. B **34**, 6819 (1986).
[28] H. C. Kang and W. H. Weinberg, J. Chem. Phys. **90**, 2824 (1989).
[29] K. A. Fichthorn and W. H. Weinberg, J. Chem. Phys. **95**, 1090 (1991).
[30] M. C. Righi, C. A. Pignedoli, R. Di Felice, C. M. Bertoni, and A. Catellani, Phys. Rev. B **71**, 075303 (2005).
[31] A. Kley, P. Ruggerone, and M. Scheffler, Phys. Rev. Lett **79**, 5278 (1997).
[32] C. Roland and G. H. Gilmer, Phys. Rev. B **46**, 13428 (1992).
[33] G. Costantini, A. Rastelli, C. Manzano, P. Acosta-Diaz, R. Songmuang, G. Katsaros, O. G. Schmidt, and K. Kern, Phys. Rev. Lett. **96**, 226106 (2006).
[34] F. Patella, S. Nufris, F. Arciprete, M. Fanfoni, E. Placidi, A. Sgarlata, and A. Balzarotti, Phys. Rev. B **67**, 205308 (2003).
[35] B. A. Joyce and D. D. Vvedensky, Mater. Sci. Eng. R. **46**, 127 (2004).